STUDIA UBB CHEMIA, LVI, 3, 2011 (p. 147 - 156)

THE INFLUENCE OF SOME SYNTHESIS CONDITIONS ON THE STRUCTURE OF CALCIUM PHOSPHATE POWDERS

MILICA TODEA[*a], TEODORA MARCU[b], MONICA TAMASAN[a], SIMION SIMON[a], CATALIN POPA[b]

ABSTRACT. Calcium phosphate powders were synthesized based on a wet chemical precipitation method at room temperature. A critical aging time of the precipitate is required in order to form a desired intermediate complex that permits a further transformation to apatite phase under appropriate thermal treatment. The processing parameters effect on apatite formation was systematically studied in terms of aging time and different condition of synthesis using Thermal Analysis, X-ray diffraction and Fourier transform infrared spectroscopy. The transformation of calcium phosphate deficient apatite (monetite and $Ca_2P_2O_7$) obtained after one and two weeks of aging time into hydroxyapatite is completed when a heat treatment is applied at 600 ^oC under air. The HA nanocrystal sizes decrease with the increase of the aging periods, from 90 to 50 nm. The results show that by suitable tailoring of the processing parameters one can obtain calcium phosphate powders of desired dimensions.

Keywords: *hydroxyapatite, nanocrystalls, DRX, FTIR, DTA.*

INTRODUCTION

Calcium phosphate is recognized to be one of the most attractive candidate materials for bone replacement since the human skeleton consists of a composite of calcium phosphate crystals with a matrix phase of collagen. Inorganic bioceramic hydroxyapatite ($Ca_{10}(PO_4)_6(OH)_2$) as the main constituent of natural bone and teeth has excellent biocompatibility and tissue bioactivity. The morphological characteristics of HA particles, such as shape, size, and size distribution play an important role in the mechanical, chemical, and biological properties of HA-based materials. The precipitation mechanism of HA follows a nucleation-aggregation-growth sequence of events [1]. In this approach, HA particles with sizes ranging from nanometric to micrometric can be obtained; from the morphological point of view they may be irregular or ordered aggregates [2]. Bone substitute materials must be actively resorbed in vivo by the osteoclasts [3] (cells that

[a] *Faculty of Physics & Institute of Interdisciplinary Research on Bio-Nano-Sciences, Babes Bolyai University, Cluj-Napoca, 400084, Romania*

[b] *Technical University of Cluj-Napoca, Faculty of Materials and Environmental Engineering, Department of Materials Science and Technology, Muncii Avenue 103-105, 400641 Cluj-Napoca, Romania*

are able to resorb the fully mineralized bone) as they are equipped with a variety of enzymes, which lower the local pH to a range of 3.9 to 4.2. This occurs via a process called cell-mediated acidification in which the host bone can deposit new bone on the resorption sites by the means of osteoblasts (cells that build the extracellular matrix and regulate its mineralization).

Several compositions containing calcium and phosphorous, like hydroxyapatite (HA, $Ca_{10}(PO_4)_6(OH)_2$), beta tricalcium phosphate (β-TCP, $Ca_3(PO_4)_2$), or their composites (biphasic calcium phosphates, BCP) have received particular attention. HA is considered to be a bioactive and non-biodegradable bone replacement material, while TCP is resorbable and significantly more soluble than HA [4, 5]. BCP ceramics were developed in order to combine the high bioactivity of Ha and the solubility characteristics of TCP in a composite material. [6].

Brushite ($CaHPO_4 \cdot 2H_2O$) is a layered structure in which the layers are held together by water molecules via hydrogen bonds. Upon heating, brushite loses its water molecules and will transform into $CaHPO_4$ (monetite) [7]. Being a relatively high solubility calcium phosphate compound, brushite is known to convert into apatite-like calcium phosphate when soaked in SBF solutions at the human body temperature for about one week [8–22].

Both brushite [23, 24] and monetite [25] phases are successfully used as starting materials in the preparation of the powder components of self-hardening apatitic calcium phosphate cements [26]. Aging of the precursor solution has been found to be critical in developing an apatitic phase. A critical aging time is required to complete reaction between Ca and P molecular precursor to form a desired intermediate complex that allows a further transformation to apatite phase under appropriate thermal treatment [27].

The main purpose of this study was to analyze systematically the influence of aging time, heat treatment and different synthesis condition (eg washing samples) on the structure of calcium phosphate samples obtained by the precipitation method at room temperature.

RESULTS AND DISCUSSION

Calcium phosphate powders were synthesized based on a wet chemical precipitation method at room temperature, with calcium nitrate and diammonium hydrogen phosphate, as detaile din the Methods section.

In order to establish the calcination temperatures, differential thermal analysis (DTA) and thermogravimetric (TG) results were used. The DTA and TGA (STA: simultaneous thermal analysis) curves for the as prepared calcium phosphate powder are displayed in Figure 1. These show, in the 35-150ºC range, an endothermic event with mass decrease of 3 % due to the loss of surface adsorbed water. A second mass decrease of about 20 % is recorded in 200-300ºC temperature range, and this is accompanied by an endothermic peak in DTA curve, with the maximum at 270ºC. Based upon the formula $CaHPO_4 \cdot 2H_2O$ the theoretical mass loss for the dehydration

of brushite is 20.93%. In our study, the experimentally determined mass loss attributed to the dehydration of brushite is around 20% in very good accord with the literature [7, 26, 29, 38]. These authors observed that brushite transformed to monetite at around 200ºC with a weight loss of 20.3% and the monetite to calcium pyrophosphate ($Ca_2P_2O_7$) transition was complete above 440ºC, with 6% weigh loss. The following reactions take place during the thermal decomposition:

$$2CaHPO_4 \cdot 2H_2O \rightarrow 2CaHPO_4 + 4H_2O$$
$$2CaHPO_4 \rightarrow Ca_2P_2O_7 + H_2O$$

In this approach, the further mass loss (around 12 %) recorded in the 400-500 temperature range with a maximum at around 440^{o}C, can be related to the monetite to $Ca_2P_2O_7$ transition (with a weigh loss of 6%) and pyrolysis of the organic component and/or residual nitrate groups occurring in the samples during the synthesis of the samples (with a weigh loss of 6%) [26, 30, 31, 38].

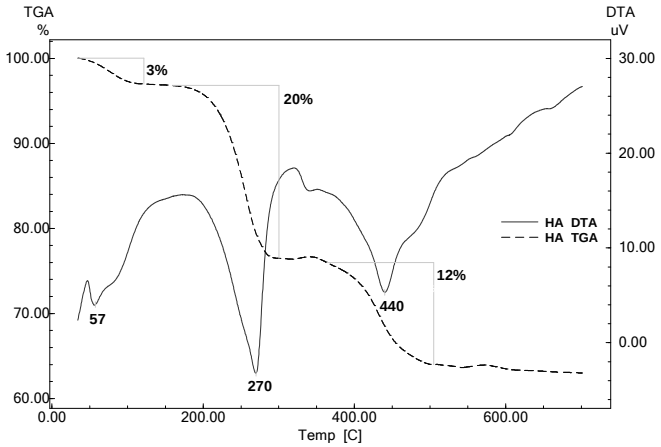

Figure 1. DTA and TG curves of as-prepared sample

The X-ray diffraction patterns for the calcium phosphate samples aged, washed and then heat treated are different in the crystalline aspect (Figs. 2 and 3). The crystalline phase identified in the as-prepared sample (0 week) is brushite. The intensity of the diffraction peaks indicated that the particles were fairly well-crystallized. As we mentioned before, by losing water during the aging periods, brushite transforms into monetite (Figure 2a). This transformation is reversible, as it can be seen in Figure 3a for the samples that were aged one or two weeks (monetite) after washing in pure water the main crystalline phase became brushite.

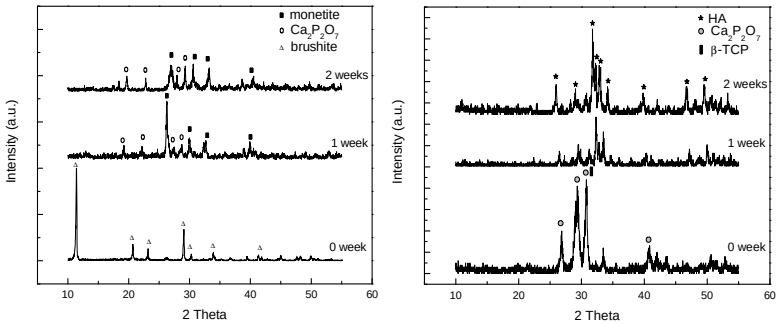

a) b)

Figure 2. *XRD patterns of the samples after different aging time periods a) not heat treated b) heat treated at 600℃*

The XRD reflection peak at 2θ = 12º is attributed to brushite powder. The average crystallites size, determined by Scherrer's formula for the peak with 2θ =12.1º for the as-prepared sample is of about 55 nm (Table 1). It is important to notice that in the washed samples the crystallites size value increases at 132 nm due to the hydration of the samples. Brushite as main crystalline phase transform into two phase mixture of calcium phosphate containing $Ca_2P_2O_7$ and a small amount of β-TCP after the heat treatment (Figure 2b).

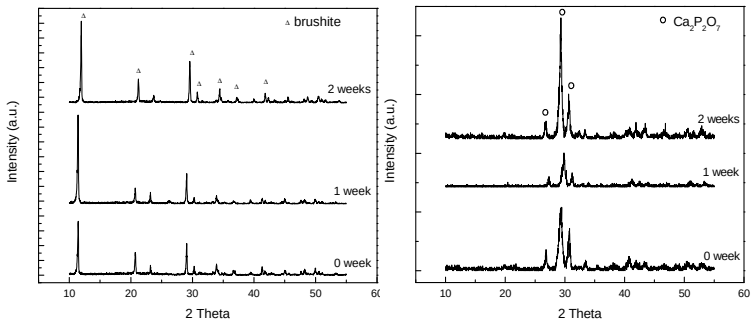

a) b)

Figure 3. *XRD patterns of the samples washed after different aging time periods a) not heat treated b) heat treated at 600℃*

This applies to not aged as-prepared samples and all samples that were washed in pure water. The crystallites size has values ranging between 35-44 nm (Table 1). Both $Ca_2P_2O_7$ and β-TCP phases are not necessarily detrimental components of bioceramics, since they provide faster than apatite dissolution rate in physiological environments [26, 27].In fact, this would be an advantage from the bioresorbtion point of view.

The transformation of calcium phosphate deficient apatite (monetite and $Ca_2P_2O_7$) obtained after one and two weeks (Figure 2a) of aging into hydroxyapatite (Figure 2b) is completed at 600 ^oC [6]. The XRD results confirm those obtained from DTA. The HA crystallites size decreases with the increase of the aging periods, from 90 to 50 nm (Table 1). The crystallite size of HA is of main importance for the biomedical application. A smaller size is expected to result in a higher bioactivity.

Table 1. Crystalline phases and corresponding crystallites size of calcium phosphate samples

Sample		Crystalline phase	2 theta[^{o}]	Crystallites size [nm]
	0 week	brushite	12.1	55
	1 week	monetite	29.9	69
		$Ca_2P_2O_7$	26.2	73
	2 weeks	monetite	30.5	83
		$Ca_2P_2O_7$	27.0	21
heat treated	0 week	$Ca_2P_2O_7$	26.8	52
		β-TCP	30.7	44
	1 week	HA	32.3	90
	2 weeks	HA	31.8	50
washed	0 week	brushite	12.1	132
	1 week	brushite	11.4	132
	2 weeks	brushite	11.9	132
washed and heat treated	0 week	$Ca_2P_2O_7$	26.8	41
		β-TCP	30.6	35
	1 week	$Ca_2P_2O_7$	26.8	36
	2weeks	$Ca_2P_2O_7$	26.3	36

FTIR measurements were performed to evaluate possible differences in the chemical composition of the calcium phosphate powders with different Ca/P ratios. The FTIR spectra of calcium phosphate powders for different aging periods before and after the heat treatment at 600^oC are presented in Figures 4 and 5. The crystalline phases identified by XRD were also confirmed by FTIR spectral analysis. The spectra of calcium phosphate samples before the heat treatment (Figure 4a) show the characteristic peaks of absorbed water, hydroxyl, phosphates and carbonate species.

The bands between 3250-3500 cm^{-1} corresponding to the O-H stretching of adsorbed water [7, 32] are broad for all the samples aged and unwashed (Figure 4a). The spectra clearly indicate a band at around 1640 cm^{-1} (bending mode), which is attributed to the presence of the adsorbed water [7]. The bands around 1135, 1060 cm^{-1} and in the range of 660- 528 cm^{-1} are characteristic for vibrational mode of phosphate group in several distinctive sites [6].

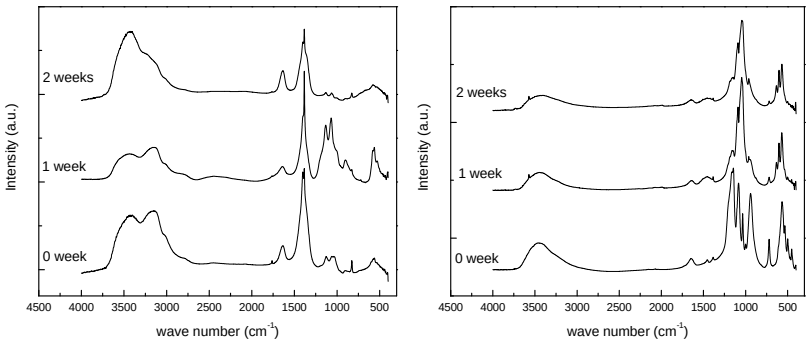

Figure 4. *FT-IR spectra of the samples after different aging time periods a) not heat treated b) heat treated at 600℃*

The XRD results show that the crystalline phases identified in these samples are monetite and $Ca_2P_2O_7$. The P-OH stretching modes in HPO_4 groups have been identified around 880 cm^{-1} [7]. The bands at 825 and 1385 cm^{-1} were attributed to residual NO_3^- groups resulting from synthesis precursors [39]. The absorption bands around 1470 cm^{-1} and 890 cm^{-1} represent an indicative of carbonate species, which is presumed to have come from the atmosphere during the aging period [32]. The total intensity of these bands decreases for the samples washed after all aging periods.
The spectra of the heat treated samples aged for one and two weeks (Figure 4b) are characteristic for calcium hydroxyapatite [2, 34]. All bands originating from PO_4 and OH groups are clearly visible. The OH vibrations at 3400-3200 cm^{-1} (stretching) are well-defined but they diminished upon heating the samples. The bands assigned to the stretching modes 3570 cm^{-1} and librational modes at 631 cm^{-1} of OH group in the hydroxyapatite, are clearly observed in the spectra [34].

The bands in the region 1650–1600 cm^{-1} are a result of H–O–H vibrational modes of adsorbed water [35, 36]. The presence of broad distinct bands in the range 1500–1400 cm^{-1} means that the HA samples contain small quantities of carbonate ions. These bands are missing from the FTIR spectra of the washed samples and then heat treated (Figure 5b). These facts confirm the elimination of the carbonate from the samples when they are washed and then heat treated. The main vibrational bands of the hydroxyapatite PO_4 groups are observed at around 1157, 1095, 1040, 960, 601 and 571 cm^{-1} for one and two weeks aged samples, after the heat treatment [32-36]. This result sustains the X-ray diffraction conclusions.

After washing, the FT-IR spectra for all the samples present bands in the same regions but they became sharper and narrower (Figure 5a). The bands at 3543, 3494, 3281, 3163 cm^{-1} and also the shoulder at around

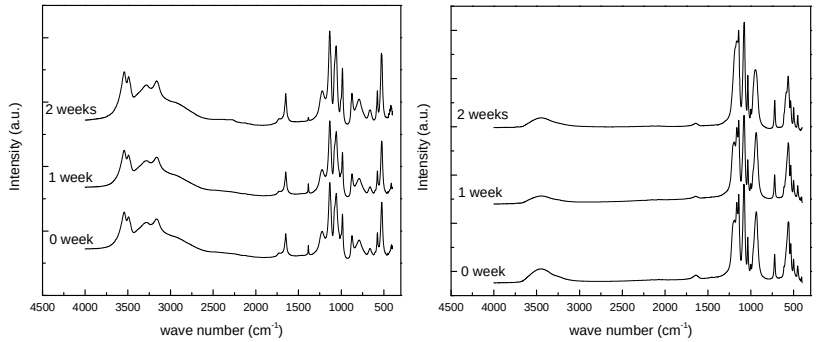

Figure 5. *FT-IR spectra of the samples washed after different aging time periods a) not heat treated b) heat treated at 600 ℃*

2955 cm^{-1} were due to the O-H stretching of water. The band at 1648 can be assigned to the bending vibration of water. Bands at 874 cm^{-1} and 1220 cm^{-1} assigned to the HPO_2^{-4} group of brushite [7,40] were observed in all the washed samples. The band at 985 cm^{-1} originated from the P-OH symmetric stretching vibration of PO_3^{4-}. In addition, the band at around 1060 cm^{-1} was attributed to the v_3 vibration of the PO_3^{4-}. Stretching vibrations of PO groups at 1136 cm^{-1} was assigned vibration of HPO_2^{-4} ions in brushite [40]. Water libration was observed for all the samples at 791 cm^{-1}. The bending vibrations of the P-O-P mode were recorded at 660, 576, 528 cm^{-1}, attributed to phosphate groups associated with brushite, the only crystalline phase present in this samples [7, 26, 33, 34, 35].

Figure 5b, referring to washed and heat treated samples, shows, as well as all of the above-mentioned bands, a unique sharp peak at around 720 cm^{-1} which is characteristic of the P–O–P vibrational mode indicating the presence of pyrophosphates ($Ca_2P_2O_7$) [37, 40]. FTIR spectra of as-prepared samples heat treated (Figure 4b) show the same feature. The results confirm the ones from XRD patterns, indicating the predominant presence of $Ca_2P_2O_7$ as a decomposition product, after heat treatment, in these samples.

CONCLUSIONS

Calcium phosphate powders were found to display different physical and chemical characteristics according to the preparing aging periods. The transformation of calcium phosphate deficient apatite (monetite and $Ca_2P_2O_7$) obtained after one or two weeks of aging into hydroxyapatite is completed only when a heat treatment is applied at 600 ^oC in air. Hydroxyapatite crystallite sizes decrease with the increase of the aging period. The two weeks aging time gave the best result in terms of HA crystallites size, as the bioactivity increase with the decrease of the grains size.

EXPERIMENTAL SECTION

Calcium phosphate powders were synthesized based on a wet chemical precipitation method at room temperature using calcium nitrate tetrahydrate ($Ca(N0_3)_2 \cdot 4H_20$) and diammonium hydrogen phosphate ($(NH_4)_2HPO_4$). All chemicals were reagent grade (Sigma Aldrich) and used without further purification. The white sol was stable and no gelation occurred over an aging period as long as several weeks. During the aging process, the pH of the sol increases from 4.5 at the beginning to 4.8 after the final aging period. Diammonium hydrogen phosphate hydrolyzed sol was added dropwise to the constantly stirred aqueous calcium nitrate solution at the molar ratio of Ca to P equal to 1.67. The mixed sol solution was then continuously stirred for about 50 min to obtain a white consistent sol with pH 4.5. The precipitate was taken at an aging time period of one and two weeks at room temperature and parts of them were washed with distilled water followed by filtration and dried at 80℃. After drying, the powders were calcinated at 600ºC, for 30minutes in air atmosphere.

Phase identification of the samples before and after calcination was performed by X-ray diffraction (XRD) with a Shimadzu XRD-6000 diffractometer, using Cu-K_α radiation (λ = 1.5418 Á), with Ni–filter. The XRD patterns were recorded in the 2θ scan range 10-80º, with a scan speed of 2º/min, using as calibrating material quartz powder. All powder samples were characterized after being lightly grinded by an agate mortar and pestle.

The crystallite size was estimated from the X-ray diffractograms using the Scherrer formula [28].

$$D = k\lambda/\beta_{1/2} \cos \theta,$$

Where D is the crystallite size (Å), k is a shape factor equal to 0.9, λ is the X-ray wavelength (1.5405 Å), θ is the diffraction angle expressed in radians, and $\beta_{1/2}$ is defined as

$$\beta_{1/2} = (B^2 - b^2)^{1/2}$$

B being the diffraction peak width at half height and b the natural width of the instrument.

Thermal analysis was conducted on a Shimadzu type derivatograph DTG-60H at a heating rate of 10ºC/min, up to 700ºC. Alumina open crucibles and α-alumina powder as reference material were used and the measurement was made in a dynamic nitrogen and air atmosphere at a flow rate of 70 ml/min.

The infrared measurements were carried out using a Bruker Equinox 55 spectrometer. The FTIR spectra were recorded on powdered samples pressed in KBr pellets, with a spectral resolution of 2 cm^{-1}, over the range of 4000 to 400 cm^{-1}.

ACKNOWLEDGMENTS

Financial support from the "Progress and development through post-doctoral research and innovation in engineering and applied sciences – PRiDE - Contract no. POSDRU/89/1.5/S/57083" project co-funded from European Social Fund through Sectorial Operational Program Human Resources 2007-2013 (to MT), project POSDRU/21/1.5/G/36154 „Performant doctoral program for the development of highly qualified human resources in the interdisciplinary scientific research", and BIOMAPIN PCCE-101/2008 (Romanian National University Research Council) is gracefully acknowledged.

REFERENCES

1. R. R. Clemente, A. L. Macipe, J. G. Morales, J. T. Burgues, and V. M. Castanho, *Journal of the European Ceramics Society*, **1998**, *18*, 1351–1356
2. M.A. Martins, C. Santos, M.M. Almeida, M.E.V. Costa, *Journal of Colloid Interface Science* **2008**, *318*, 210-216
3. F Monchau; A Lefèvre; M Descamps; A Belquin-myrdycz; P Laffargue; H FHildebrand, *Biomolecular Engineering*, **2002**,*19(2-6)*,143-152
4. C. P. A. T. Klein, A. A. Driessen, K. Groot, and A. Hoof, *Journal of Biomedical Materials Research*, **1983**, *17*, 769-784
5. P. Ducheyne, S. Radin, L. King, *Journal of Biomedical Materials Research,* **1993**, *27*, 25-34
6. J. Marchi, P. Greil, J.C.Bressiani, A. Bressiani, F. Muller, *International Journal of Applied Ceramic Technology*, **2009**, *6*, 60-71
7. S. Mandel, A.C. Tas, *Materials Science and Engineering C* **2010**, *30*, 245–254
8. D. Walsh, J. Tanaka, *Journal of Materials Science: Materials in Medicine*, **2001**, *12*, 339-343
9. S.J. Lin, R.Z. LeGeros, J.P. LeGeros, *Journal of Biomedical Materials Research* **2003**, *66A*, 819-828
10. H.S. Azevedo, I.B. Leonor, C.M. Alves, R.L. Reis, *Materials Science and Engineering: C* **2005**, *25*, 169-179
11. Lu X and Leng Y, *Biomaterials*, **2005**, *26*, 1097-1108
12. Zainuddin, Hill DJT, Traian CV, Whittaker AK, Kemp A. *Biomacromolecules*, **2006**, *7(6)*, 1758-1765
13. M. Kumar, H. Dasarathy, C. Riley, *Journal of Biomedical Materials Research* **1999**, *45*, 302-310
14. C.Y. Kim, H.B. Lim, *Key Engineering Materials*, **2004**, *254-256*, 305-310
15. J.A. Juhasz, S.M. Best, A.D. Auffret, W. Bonfield, *Journal Of Materials Science: Materials in Medicine* **2008**, *19*, 1823-1829

16. J. Pena, I. Barba-Izquierdo, A. Martinez, M. Vallet-Regi, *Solid State Sci.* **2006**, *8*, 513-519
17. Y. Honda, S. Kamakura, K. Sasaki, T. Anada, T. Masuda, O. Suzuki, *Key Engineering Materials*, **2007**, *330–332*, 479-482
18. R. Gildenhaar, G. Berger, E. Lehmann, C. Knabe, *Key Engineering Materials*, **2008**, *361–363*, 331-334
19. L. Grondahl, F. Cardona, K. Chiem, E. Wentrup-Byrne, T. Bostrom, *Journal of Materials Science: Materials in Medicine* **2003**, *14*, 503-510
20. A. Rakngarm, Y. Mutoh, *Materials Science and Engineering: C,* **2009**, *29(1)*, 275 - 283
21. F. Yang, J.G.C. Wolke, J.A. Jansen, *Chemical Engineering Journal*, **2008**, *137*, 154-161
22. L.P. Xu, E.L. Zhang, K. Yang*, Journal of Materials Science: Materials in Medicine,* **2009**, *20*, 859-867
23. K. Kurashina, H. Kurita, M. Kotani, C.P.A.T. Klein, K. de Groot, *Biomaterials*, **1997**, *18*, 539-543
24. D. Knaack, M. E. P. Goad, M. Aiolova, C. Rey, A. Tofighi, P. Chakravarthy and D. D. Lee, *The Journal of Biomedical Materials Research*, **1998**, *43(4)*, 399-409
25. E.M. Ooms, J.G.C. Wolke, M.T. van de Heuvel, B. Jeschke and J.A. Jansen, *Biomaterials* **2003**, *24*, 989–1000
26. A. C. Tas and S. B. Bhaduri, Bioceramics: Materials and Applications V, Ceramic Transactions, Vol. **164**, pp. 119-128, (Eds.) V. Sundar, R. P. Rusin, and C. A. Rutiser, The American Ceramic Society, 2004, USA, ISBN 1-57498-185-4.
27. D-M. Liu, T. Troczynski, W. J. Tseng, *Biomaterials* **2002**, *23*, 1227-1236
28. T.J. Burgues, R.R. Clemente, *Crystal Research and Technology,* **2001**, *36*, 1075-1082
29. A. Dosen and R.F. Giese, *American Mineralogist*, **2011**, *96*, 368-373
30. M. Mozafari, F. Moztarzadeh, M. Tahriri, *Journal of Non-Crystalline Solids*, **2010**, *356*, 1470–1478
31. I. Bogdanoviciene, A. Beganskiene, K. Tonsuaadu, J.Glaser, H.Juergen. Meyer, A. Kareiva, *Materials Research Bulletin* , **2006**, *41*, 1754–1762
32. T.V. Thamaraiselvi, K. Prabakaran and S. Rajeswari, *Biomaterials and Artificial Organs*, **2006**, *19*, 81-83
33. N. Temizel, G. Girisken, and A. C. TAS, *Materials Science and Engineering C: Materials for Biological Applications*, **2011**, *31(5)*, 1136-1143
34. Soon-Ho Kwon, Youn-Ki Jun, Seong-Hyeon Hong, Hyoun-Ee Kim, *Journal of the European Ceramic Society,* **2003**, *23,* 1039–1045
35. X. Bai, K. More, C.M. Rouleau, A. Rabiei, *Acta Biomaterialia*, **2010**, *6*, 2264-2273
36. A. C. Tas, *Biomaterials*, **2000**, *21 (14)*, 1429-1438
37. A. C. Tas, *Journal of The American Ceramic Society*, **2001**, *84 (2)*, 295-300
38. R. L. Frost and S. J. Palmer*, Thermochimica Acta*, **2011**, *521*, 14-17
39. D.K. Pattanayak, R. Dash, R.C. Prasad, B.T. Rao, T.R. Rama Mohan, *Materials Science and Engineering: C*, **2007**, *27*, 684-690
40. J. P. Maity, Tz-J. Lin, H. P-H Cheng, C-Y. Chen, A. S. Reddy, S.B. Atla, Y-F. Chang, H-R. Chen and C-C Chen, *International Journal of Molecular Sciences*, **2011**, *12*, 3821-3830